Bimolecular Crystals of Fullerenes in Conjugated Polymers and the Implications of Molecular Mixing for Solar Cells

By *A. C. Mayer, Michael F. Toney, Shawn R. Scully, Jonathan Rivnay, Christoph J. Brabec, Marcus Scharber, Marcus Koppe, Martin Heeney, Iain McCulloch,* and *Michael D. McGehee**

The performance of polymer:fullerene bulk heterojunction solar cells is heavily influenced by the interpenetrating nanostructure formed by the two semiconductors because the size of the phases, the nature of the interface, and molecular packing affect exciton dissociation, recombination, and charge transport. Here, X-ray diffraction is used to demonstrate the formation of stable, well-ordered bimolecular crystals of fullerene intercalated between the side-chains of the semiconducting polymer poly(2,5-bis(3-tetradecylthiophen-2-yl)thieno[3,2-*b*]thiophene. It is shown that fullerene intercalation is general and is likely to occur in blends with both amorphous and semicrystalline polymers when there is enough free volume between the side-chains to accommodate the fullerene molecule. These findings offer explanations for why luminescence is completely quenched in crystals much larger than exciton diffusion lengths, how the hole mobility of poly(2-methoxy-5-(3′,7′-dimethyloxy)-p-phylene vinylene) increases by over 2 orders of magnitude when blended with fullerene derivatives, and why large-scale phase separation occurs in some polymer:fullerene blend ratios while thermodynamically stable mixing on the molecular scale occurs for others. Furthermore, it is shown that intercalation of fullerenes between side chains mostly determines the optimum polymer:fullerene blending ratios. These discoveries suggest a method of intentionally designing bimolecular crystals and tuning their properties to create novel materials for photovoltaic and other applications.

1. Introduction

Bulk heterojunction (BHJ) solar cells based on a blend of an electron donor polymer (such as regioregular poly(3-hexylthiophene) (P3HT) or poly(2-methoxy-5-(3′,7′-dimethyloxy)- *p*-phylene vinylene) (MDMO-PPV)) and an electron accepting fullerene (either phenyl-c61-butyric acid methyl ester ($PC_{[61]}BM$) or phenyl-c71-butyric acid methyl ester ($PC_{[71]}BM$)) have received considerable attention recently due to a reported power conversion efficiency around 5% along with the promise of low-cost production.[1–6] The performance of BHJs is heavily influenced by the interpenetrating nanostructure formed by the two semiconductors because exciton dissociation, recombination and charge transport are all affected by the size of the phases, the nature of the interface and molecular packing. The specific nanostructure morphology is a result of the interplay between the thermodynamics of the blend, which arise from the nature of the intermolecular bonds and determine the equilibrium state, and the kinetics of film formation, which determine the approach to equilibrium. Despite much work in this area, most BHJ design is highly empirical. A variety of polymer:fullerene BHJ solar cells have been explored and it has been found that some systems optimize with a blend ratio around 1:1 by weight, but most optimize closer to 1:4 by weight. Little is known about what material properties are responsible for determining the optimal blend ratio. It is known that the optimal 1:4 MDMO-PPV:$PC_{[61]}BM$ system contains $PC_{[61]}BM$ domains surrounded by a phase that is composed of the polymer and the fullerene intimately mixed at the molecular level.[6] In P3HT:$PC_{[61]}BM$ solar cells, the materials are thought to separate

[*] Prof. M. D. McGehee, Dr. A. C. Mayer, Dr. S. R. Scully, J. Rivnay
Department of Materials Science and Engineering
Stanford University
Stanford, CA 94305 (USA)
E-mail: mmcgehee@stanford.edu
Dr. M. F. Toney
Stanford Synchrotron Radiation Laboratory
Menlo Park, CA 94025 (USA)
Dr. C. J. Brabec, Dr. M. Scharber, M. Koppe
Konarka Technologies Austria
Altenbergerstrasse 69
4040 Linz (Austria)
Prof. M. Heeney
Department of Materials
Queen Mary, University of London
London E1 4NS (UK)
Prof. I. McCulloch
Department of Chemistry
Imperial College
London SW7 2AZ (UK)

DOI: 10.1002/adfm.200801684

© 2009 WILEY-VCH Verlag GmbH & Co. KGaA, Weinheim

into phases of nearly pure polymer and pure fullerene. For most combinations of material that have been used to make BHJ solar cells, little is known about whether the molecules mix at the molecular level (and how they mix) or if they phase separate. There are no design rules to predict when the fullerene will mix with the polymer on the molecular scale and when large-scale phase separation will occur, despite the importance that mixing has on exciton harvesting and charge recombination.

A bimolecular crystal is a structure wherein two distinct chemical species arrange in an ordered, thermodynamically stable arrangement. Such crystals of organic molecules have been observed for nonlinear optical systems of hydrogen bonded networks[7,8] as well as between semiconducting molecules and inorganic dopants such as iodine in pentacene and iodine in P3HT.[9] Enhanced p-type conductivity was recently reported for an inorganic analogue of binary nanocrystal superlattices.[10] Similarly, bimolecular crystals of semiconducting molecules may give rise to new useful electronic properties such as strong charge-transfer states due to the strong coupling of the dissimilar nearest neighbor molecules.

Poly(2,5-bis(3-tetradecyllthiophen-2-yl)thieno[3,2-*b*]thiophene) (pBTTT) is a well-ordered semicrystalline polymer that is attractive for BHJ solar cells because of its high charge carrier mobility (0.2 to 0.6 $cm^2 V^{-1} s^{-1}$) and ideal for studies that probe the molecular order of nanostructures because intense highly peaked diffraction patterns arise when films are probed with X-rays.[11–14] Pristine films of pBTTT, like P3HT, are composed of semi-crystalline lamellae separated by insulating alkyl chains,[11] however films of pBTTT have a higher degree of crystallinity and order than films of P3HT because interdigitation of side-chains from adjacent lamellae (Fig. 1a) occurs in pBTTT.[12] One might expect that BHJs containing pBTTT would suffer from poor exciton harvesting as the pBTTT could form large crystals that would expel the fullerene. However, we recently showed that the photoluminescence of pBTTT is completely quenched with the addition of fullerene molecules, which implies that exciton harvesting is efficient.[14] We found that 1:4 blends had a cell efficiency of 2.35%, while the 1:1 blends had a surprisingly low efficiency of only 0.16%.[14]

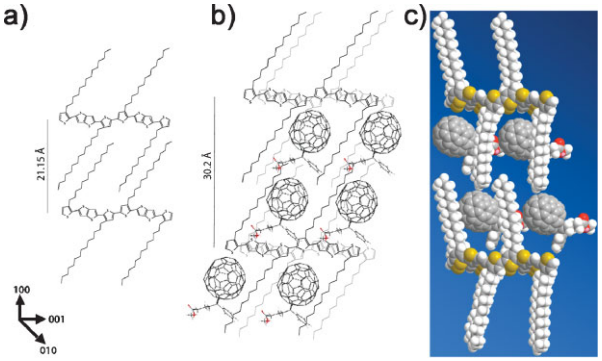

Figure 1. Schematic of possible structures showing the effect of $PC_{[71]}BM$ intercalation on the crystal lattice of pBTTT. a) The tilt angle for the pristine pBTTT crystal and the amount of interdigitation of the side-chains is set to make the d-spacing agree with X-ray diffraction and the literature [8,11]. b) The $PC_{[71]}BM$ is placed within the intercalated pBTTT:$PC_{[71]}BM$ in order to agree with the d-spacings found in X-ray scattering. c) The total volume taken up by the electron orbitals using a space-filling routine from ChemBio3D Ultra shows that there is still sufficient room for the intercalation demonstrated in (b). The tilt of the side-chains in (c) is only approximate because the simulations do not account for intermolecular interactions. The lattice axes are shown in the lower left corner for reference.

In this article, we show that the origin of the optimal 1:4 blending ratio in pBTTT:$PC_{[71]}BM$ blends predominantly results from fullerene intercalation into the polymer crystal forming highly ordered bimolecular crystals (Fig. 1b). Such crystals had not been observed before with materials used to make solar cells. Long thermal anneals and X-ray diffraction show that the bimolecular crystals are thermodynamically stable with approximately one monomer to one fullerene. The intercalation of the fullerene limits electron transport in 1:1 blends since there is no phase separation and therefore no pure electron transporting phase. X-ray diffraction and ambipolar thin-film transistor (TFT) measurements show that as the amount of fullerene is increased beyond ~50%, phase separation occurs and continuous pathways for electron transport form. We rationalize fullerene intercalation through an analysis of the three dimensional sizes and shapes of the molecules which shows that fullerene molecules are small enough to fit between the polymer's tetradecyl side-chains. We further show that fullerene intercalation occurs for other polymers and is likely to occur in blends with both amorphous and semicrystalline polymers when there is enough free volume between the side-chains to accommodate the fullerene molecule. These discoveries suggest a method of intentionally designing bimolecular crystals and tuning their properties to create novel materials for photovoltaic and other applications and offer explanations for various long-standing questions such as:

i) How can luminescence be completely quenched on ultrafast timescales when polymer crystals/domains are larger than exciton diffusion length?
ii) How does the hole mobility of MDMO-PPV films increase by over 2 orders of magnitude when fullerene derivatives are added?
iii) Why does large-scale phase separation occur in some polymer: fullerene blend ratios while thermodynamically stable mixing on the molecular scale occurs for others?
iv) What microscopic mechanism determines the optimum polymer:fullerene blending ratios?

2. Results and Discussion

Figure 2 shows X-ray scattering of pBTTT:$PC_{[71]}BM$ blends of varying weight ratio that have been annealed at 185 °C for 10 minutes. The annealing took place at the glass transition temperature of pBTTT in order to increase the molecular order. The 2D grazing incidence X-ray scattering (2D GIXS) for a pristine pBTTT film (Fig. 2a) is consistent with the literature and displays several diffraction orders along the vertical slice at $q_{||} \approx 0$, which is deviated from true specular ($q_{||} = 0$) due to the scattering geometry (see Ref. [13] for details). These peaks are denoted as $(100)_p$, $(200)_p$, etc. and correspond to a lamellar d-spacing of 21.15 Å. The subscript "p" refers to the pristine pBTTT lattice. The scattering for pristine pBTTT also exhibits 2 broad vertical streaks at a $q_{||}$ equal to 1.41 $Å^{-1}$ and 1.71 $Å^{-1}$ corresponding to the

WILEY InterScience DISCOVER SOMETHING GREAT
© 2009 WILEY-VCH Verlag GmbH & Co. KGaA, Weinheim

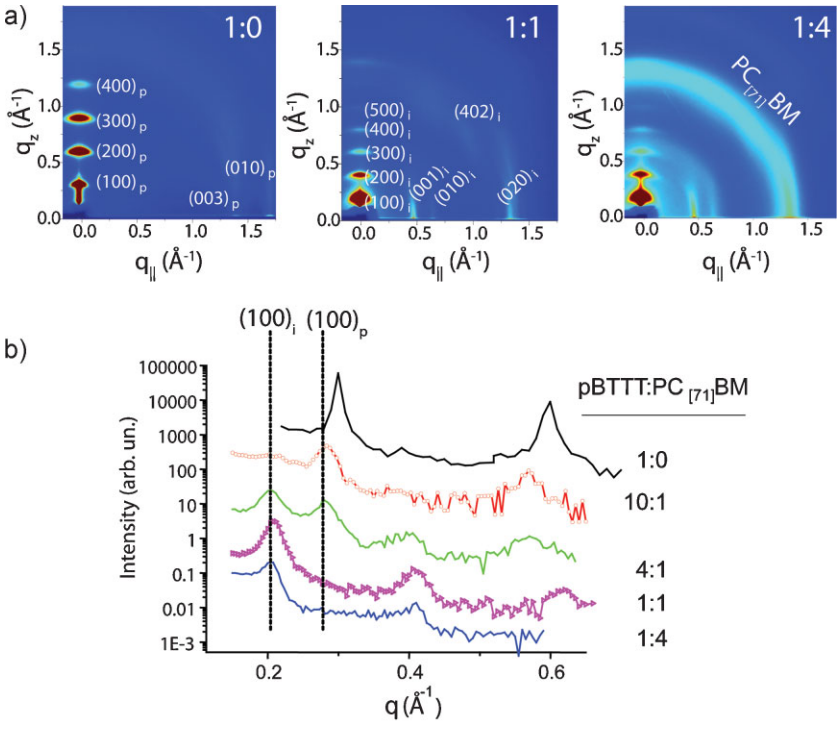

Figure 2. X-ray scattering spectra of annealed pBTTT:PC$_{[71]}$BM films with varying weight ratios demonstrating the intercalation of the PC$_{[71]}$BM into the pBTTT lattice. a) The 2D grazing incidence X-ray scattering of a pristine film, a 1:1 pBTTT:PC$_{[71]}$BM blend, and a 1:4 pBTTT:PC$_{[71]}$BM blend demonstrates an expansion of the crystal lattice with the introduction of PC$_{[71]}$BM. b) High-resolution specular X-ray diffraction confirms the expansion perpendicular to the substrate. The specular scan for the pristine film (black line) is consistent with the literature for a highly ordered crystal with interdigitated side-chains. The specular scan for the 10:1 blend (red line) shows a reduced shifted peak that comes from PC$_{[71]}$BM interrupting the pBTTT lattice. The X-ray diffraction for the 4:1 (green line) shows a coexistence of the pBTTT lattice as well as the intercalated lattice. The scans for the 1:1 (purple line) and the 1:4 (blue line) correspond to the expanded lattice, while the 1:4 also contains a halo representing a pure PC$_{[71]}$BM phase.

intramolecular (003)$_p$ and the π-stacking (010)$_p$, respectively.[13] This diffraction pattern has been used to show that the crystals are highly ordered and oriented with interdigitated side-chains (Fig. 1a).[11–13,15]

The 2D GIXS pattern for a 1:1 pBTTT:PC$_{[71]}$BM blend, also shown in Figure 2a, is different from the pattern for the pristine film in that the peaks along the vertical slice at $q_{||} \approx 0$ are shifted and now correspond to a d-spacing of 30.2 Å. The 2D GIXS pattern for a 1:1 pBTTT:PC$_{[61]}$BM blend (Fig. S1, Supporting Information) displays the same expansion of the lattice. We attribute the ≈9 Å increase in the d-spacing of the lamellae to the intercalation of the PC$_{[71]}$BM between the side-chains of the pBTTT. A schematic of pBTTT and PC$_{[71]}$BM drawn to scale (Fig. 1b) demonstrates how the side-chain spacing along the polymer backbone allows for this. There is one fullerene molecule per polymer monomer in the unit cell. Figure 1c shows a space-filling schematic made with ChemDraw3D. We denote the peaks of the intercalated phase with a subscript 'i'. There are several new streaks that appear along $q_{||}$ with the strongest at 0.49 and 0.667 Å^{-1} and a broad, mixed index peak at $q_{||} = 1$ Å^{-1} and $q_z = 0.81$ Å^{-1}. High resolution grazing incidence X-ray diffraction (Fig. S2, Supporting Information) for several blends corroborates the peak positions. A preliminary unit cell for the bimolecular crystal can be assigned based on the diffraction data: a triclinic lattice with $a = 30$ Å, $b = 9.9$ Å, $c = 13.5$ Å, $\alpha = 72°$, $\beta \approx 90°$, and $\gamma \approx 90°$. The reported unit cell for pBTTT is an orthorhombic one with $a = 22.15$ Å, $b = 3.67$ Å, and $c = 13.37$ Å,[13] although it appears the lattice is actually triclinic with $a = 19.6$ Å, $b = 5.4$ Å, $c = 13.6$ Å, $\alpha = 136°$, $\beta = 84°$, and $\gamma = 86°$.[16] The peak positions for the pristine lattice and the intercalated lattice are listed in Table 1. The preliminary bimolecular lattice preserves the intramolecular (*c* axis) spacing, as required. There is a doubling along the *b* axis due to the presence of the PCBM and hence there are two polymer molecules along the *b* direction. It is likely that there is an alternating π-stacking spacing in the pBTTT due to the fullerene. An exact determination of the unit cell will require orienting the crystals in every direction and is beyond the scope of this article.

The 2D GIXS pattern for the 1:4 pBTTT:PC$_{[71]}$BM blend contains the peaks that we associate with the intercalated lattice as well as an additional halo around 1.4 Å^{-1}. This halo corresponds to a pure amorphous PC$_{[71]}$BM phase that arises when phase separation occurs.[17] The absence of the fullerene halo in the 2D GIXS pattern for the 1:1 blend is additional evidence for the fullerene being mixed with the polymer at the molecular level in that blend.

High-resolution specular X-ray diffraction measurements were taken as a function of blending ratio in order to get a more complete

Table 1. X-ray diffraction peaks and indices for pristine pBTTT and pBTTT:PC$_{[71]}$BM films annealed at 185 °C for 10 minutes. The full width at half max (FWHM) was determined from a Gaussian fit after background subtraction. The (031)$_i$, (0–22)$_i$, (0–32)$_i$, and (005)$_i$ peaks were too weak to accurate measurements of the FWHM.

Film and X-ray setup	Index	Q (Å^{-1})	FWHM (Å^{-1})
pBTTT			
specular	(100)$_p$	0.299	0.08
	(200)$_p$	.598	0.08
in-plane	(003)$_p$	1.41	0.174
	(010)$_p$	1.712	0.135
pBTTT:PC$_{[71]}$BM			
specular	(100)$_i$	0.2077	0.0117
	(200)$_i$	0.4077	0.0178
	(300)$_i$	0.616	0.018
in-plane	(001)$_i$	0.489	0.041
	(010)$_i$	0.667	0.0375
	(020)$_i$	1.36	–
	PC$_{[71]}$BM	1.4	0.157
	PC$_{[71]}$BM	1.85	0.44
	(031)$_i$/(0–22)$_i$	1.88	–
	(0–32)$_i$/(005)$_i$	2.4	–

© 2009 WILEY-VCH Verlag GmbH & Co. KGaA, Weinheim

WILEY InterScience® DISCOVER SOMETHING GREAT

understanding of the nature of the intercalated crystal. The specular scans in Figure 2b demonstrate the shift in the lattice perpendicular to the substrate as $PC_{[71]}BM$ is added. The specular X-ray pattern for the pristine pBTTT film (black line, Fig. 2b) shows that the d-spacing is 21.15 Å. The scan of the 10:1 pBTTT:$PC_{[71]}BM$ blend (red line, Fig. 2b) shows both a reduction in the peak intensity and a slight shift of the d-spacing to 22.1 Å. This reduction and shift implies a reduction in the extent of ordering of pBTTT crystal caused by the introduction of the $PC_{[71]}BM$ molecules. The scan for the 4:1 blend (green line, Fig. 2b) shows the reduced and shifted peak of the 10:1, but a new peak emerges with an expanded d-spacing of 30.2 Å. This expanded lattice was observed in the 2D GIXS images of the 1:1 and 1:4 and is due to the fullerene intercalated into the lamellar stack (Fig. 1b). With the addition of more fullerene, the peak corresponding to the intercalated lattice increases in intensity and the peak associated with the 22.1 Å is completely suppressed with a blending ratio of 1:1. The existence of two sets of peaks in the 4:1 film suggests that the fullerenes are not distributed uniformly throughout the film. It is likely that once fullerenes start to intercalate in a region it is easier for additional fullerenes to intercalate into that region since the polymer chains are farther apart. Moving to a 1:4 blend does not cause any further shift of the peaks, so we conclude that the intercalated phase is complete with approximately one fullerene to one monomer and that any additional $PC_{[71]}BM$ phase separates out into pure domains as mentioned above.

The intercalation of $PC_{[71]}BM$ into the pBTTT lattice should have an effect on hole and electron transport as both the lattice is changed and the fullerene molecules are trapped within the polymer crystal. We have determined the effects on charge transport for holes and electrons using top-contact thin-film transistors (TFTs). The TFTs were fabricated by spin-casting films of varying blend ratios on a highly-doped Si substrate with an octadecyltrichlorosilane (OTS)-treated 300-nm-thick thermally grown SiO_2 dielectric layer. Some of these films were annealed at 185 °C for 10 minutes in order to enhance ordering. The mobilities are shown in Figure 3 and represent the average of several devices. The analysis is described in the methods section with typical transfer curves for some blends and the output curves for the 1:4 pBTTT:$PC_{[71]}BM$ (Fig. S4, Supporting Information) demonstrating typical ambipolar behavior for polymer:fullerene blends.[18,19] Our values of 0.068 and 0.23 $cm^2 V^{-1} s^{-1}$ for as-spun and annealed pristine films, respectively, are consistent with the literature.[11] For films with up to 50% $PC_{[71]}BM$, the hole mobility of the intercalated phase is slightly lower than that of the as-spun pristine film and no n-type behavior is exhibited (Fig. 3). When more than 50% $PC_{[71]}BM$ is added, the p-type mobility continues to drop to ~0.02 $cm^2 V^{-1} s^{-1}$ and the electron mobility of the as-spun films is highly dependent on the blending ratio going from 3.2×10^{-5} to 1.2×10^{-3} $cm^2 V^{-1} s^{-1}$ as the ratio is increased from 50% to 80% $PC_{[71]}BM$. Both the drop in p-type mobility and the rise in n-type mobility with increasing $PC_{[71]}BM$ can be described by the $PC_{[71]}BM$ phase separating out into a pure phase, which limits the pathways for hole transport and increases the pathways for electron transport. The n-type mobility at 80% $PC_{[71]}BM$ is similar to what has been reported for n-type mobility in a 1:1 P3HT:$PC_{[61]}BM$ blend,[18] probably because the 1:4 blends have equal portions of the intercalated phase and the pure fullerene phase. Annealing the blends with pure $PC_{[71]}BM$ domains causes a reduction in the n-type mobility because the free $PC_{[71]}BM$ aggregates, creating discontinuous pathways.[17] Figure S5 of the Supporting Information compares optical microscopy images of the as-spun and annealed 2:1, 1:1, and 1:4 TFTs and shows that the fullerene aggregates form only in the annealed 1:4 film.

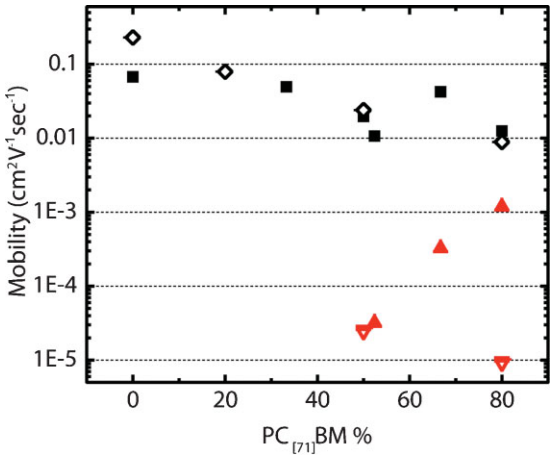

Figure 3. The effect of $PC_{[71]}BM$ intercalation on the charge transport in pBTTT:$PC_{[71]}BM$ blends as measured in an ambipolar thin film transistor as a function of $PC_{[71]}BM$-loading. The hole mobility of the as-spun blends is shown by the solid squares, while that of the annealed blends is given by open diamonds. There is no electron transport below 50% $PC_{[71]}BM$, but the electron mobility (solid triangles) increases exponentially above this value. The electron mobility of the annealed blends (open triangles) is the same as the as-spun films for $PC_{[71]}BM$-loading before the intercalated phase is completed, but is reduced for the 1:4 blend due to aggregation of the free $PC_{[71]}BM$ (see Fig. S4, Supporting Information).

Now we show that fullerenes intercalate between the side-chains of other semicrystalline polythiophenes. It was previously suggested that intercalation of $PC_{[61]}BM$ occurred in between the side-chains of poly(terthiophene) (pTT), which has enough space between its hexyl side chains to incorporate a fullerene.[20] Pristine films of pTT have a high degree of order that stems from interdigitation of the side-chains. X-ray diffraction of $PC_{[61]}BM$ blended with pTT having hexyl side-chains showed a suppression of the diffraction, rather than a shift to a larger d-spacing. The authors interpreted this data as suggesting that the fullerene disrupted the interaction between the polymer chains and prevented crystal formation. Here we show that fullerenes can intercalate between the side chains of pTT with longer dodecyl side-chains and that a bimolecular crystal forms as shown in the inset to Figure 4a. The X-ray pattern in this figure shows that upon intercalation there is a ~9 Å shift in the d-spacing for a 1:1 blend of pTT and $PC_{[61]}BM$. It is likely that the bimolecular crystal forms with the longer side-chains because the fullerene does not completely fill the space between the side-chains and leaves room for side-chain interdigitation.

The highly crystalline poly[5,58-bis(3-alkyl-2-thienyl)-2,28-bithiophene)] (PQT) also has sufficient room for intercalation, as shown in the inset to Figure 4b. It has been reported that BHJ solar cells based on blends of PQT and $PC_{[61]}BM$ demonstrated poor performance.[21] The low performance was ascribed to large

WILEY InterScience DISCOVER SOMETHING GREAT
© 2009 WILEY-VCH Verlag GmbH & Co. KGaA, Weinheim

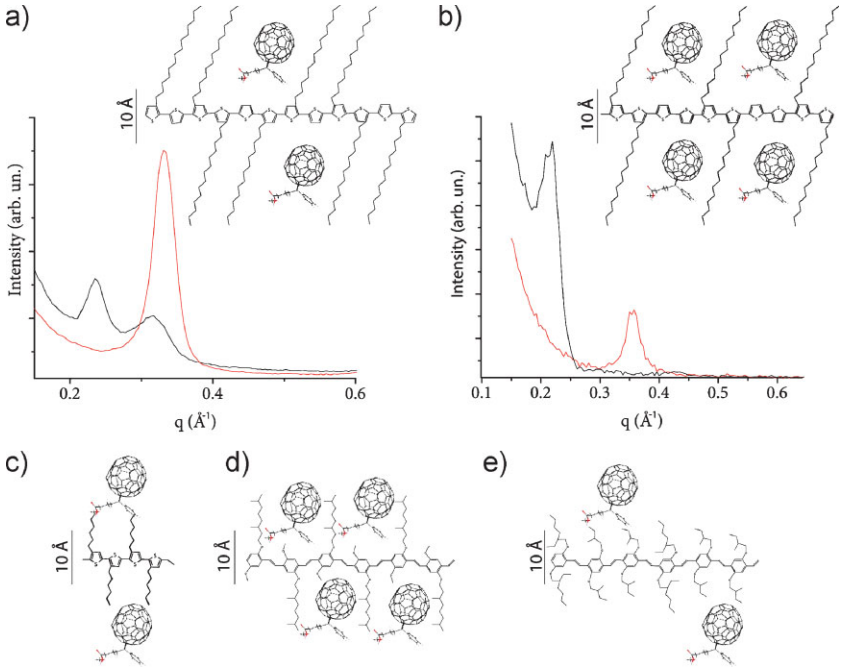

Figure 4. Fullerene intercalation in other polymer:fullerene systems. a) The X-ray diffraction pattern demonstrates an expansion of the d-spacing of the pTT (red line) upon the addition of $PC_{[61]}BM$ (black line) and the inset shows how the $PC_{[61]}BM$ fits between the side chains. b) The same situation exists for PQT as demonstrated by the X-ray pattern. c) There is insufficient room between the side-chains of P3HT to allow for intercalation. d) There is sufficient room for $PC_{[61]}BM$ intercalation between the side-chains in for amorphous MDMO-PPV. e) $BisOC_{10}$-PPV, however, does not have sufficient room.

crystal formation that expelled the $PC_{[61]}BM$. X-ray diffraction of annealed PQT and 1:1 PQT:$PC_{[61]}BM$ blend films shows an expansion of the d-spacing (Fig. 4b) with the addition of fullerenes. This expansion suggests that the fullerene actually intercalates between the side-chains of PQT. To confirm that the poor solar cell performance is not a consequence of excitons failing to reach the fullerenes due to the presence of large polymer crystals, we performed photoluminescence measurements and found that essentially all of PQT's luminescence was quenched with the addition of 20% fullerene. This example illustrates how critically important it is to know whether or not molecules mix at the molecular scale in solar cells.

In contrast to the polymers just described, 1:1 P3HT:$PC_{[61]}BM$ blends show no expanded d-spacing compared to pristine P3HT films.[2,20,22] Chemical structures drawn to scale show that there is insufficient room between the polymer side-chains for intercalation to occur (Fig. 4c). However, intercalation of iodine has been observed in between the side-chains of P3HT. Iodine intercalation can occur because iodine molecules are smaller than 6 Å. The intercalation of iodine into P3HT is thought to occur with one iodine molecule per two thiophene rings because iodine is small and it interacts very strongly with the polymer.[9] These results suggest that intercalation is related to the size of the intercalant and the side-chain spacing along the polymer backbone for various polythiophenes (Figs. 1 and 4).

Now we consider the possibility that fullerenes reside in the space between the side-chains of amorphous polymers such as MDMO-PPV. Such cases are harder to study because there are no sharp X-ray diffraction peaks to examine. Nonetheless, we argue that mixing at the molecular scale is probable when there is enough space between the side-chains to accommodate the fullerenes. In Figure 4d we show the chemical structure of MDMO-PPV stretched out in its planar confirmation. There is enough space for the fullerene to insert between the side-chains. Further work will be required to determine the exact three dimensional conformation of the polymer with and without fullerenes. Cross-sectional scanning electron micrographs have revealed that there is intimate mixing of MDMO-PPV and fullerene in a 1:1 blend, but that pure fullerene domains exist in the 1:2 MDMO-PPV:$PC_{[61]}BM$.[23] Scanning transmission X-ray microscopy has revealed that 1:4 MDMO-PPV:$PC_{[61]}BM$ blend consists of pure $PC_{[61]}BM$ domains surrounded by a 45:55 weight percent mixed phase skin layer.[24] Our intercalation model predicts that intimate mixing should occur with little phase separation until a $PC_{[61]}BM$ concentration of ~64%, which is the concentration needed to fill all of the spots between the side-chains. Blom and coworkers found that the hole mobility increased from $5 \times 10^{-7}\,cm^2\,V^{-1}\,s^{-1}$ to $\sim 1.4 \times 10^{-4}\,cm^2\,V^{-1}\,s^{-1}$ as the fullerene concentration increased from 0 to 66.7%. Additional loading of fullerene had little effect. They attributed this phenomenal increase in hole mobility, despite dilution of the polymer, to the fullerenes uncoiling the polymer chains, but were unable to provide a detailed structural picture due to the amorphous nature of the polymer. They did not observe a large increase in hole mobility upon fullerene-loading of the random co-polymer poly[2,5-bis(2-ethylhexyl-oxy)-*co*-2,5-bis (methylbutyloxy)-1,4-phenylene vinylene] (BEH-BMB-PPV), which has symmetric side-chains (Fig. 4e). Their explanation for this observation was that BEH-BMB-PPV is not coiled in the pristine film due to the symmetric nature of the side-chains.[6] We now suggest that charge transport changes dramatically when MDMO-PPV is exposed to fullerenes because the fullerenes reside between the side-chains and therefore change the intermolecular packing substantially. This notion is supported by the observation that the increase in mobility stops at ~65% fullerene loading, which is the concentration at which additional fullerene starts to go into a separate phase. We suggest that the fullerene cannot raise the mobility of BEH-BMB-PPV simply because there is no space between the side-chains to allow mixing at the molecular scale as shown in Figure 4e.

In BHJ solar cells, where the hole and electron mobilities are reasonably matched, it is believed that the primary source of recombination is geminate.[6] Peumans has performed Monte Carlo simulations on BHJs with various donor:acceptor volume ratios and found that electrons and holes are most likely to escape from each other when the volumes are matched.[25] In his model the donor and acceptor phases were assumed to consist of only one material. When the volume ratio deviates far from 1:1,

© 2009 WILEY-VCH Verlag GmbH & Co. KGaA, Weinheim

Table 2. Fullerene intercalation in a variety of polymer:$PC_{[61]}BM$ systems. The molecular weights are 910.9 and 1 031 g mol^{-1} for $PC_{[61]}BM$ and $PC_{[71]}BM$, respectively. The number of monomers to fullerenes is determined from schematics similar to Figure 4. APFO-Green5 is an alternating polyflurorene [26] and PCPDTBT is poly[2,6-(4,4-bis-(2-ethylhexyl)-4H-cyclopenta[2,1-*b*;3,4-b′]dithiophene)-*alt*-4,7-2,1,3-benzothiadiazole]] [27].

Polymer	M_w of monomer g mol^{-1}	Monomers/ Fullerene	Ideal % $PC_{[61]}BM$ (Ideal % $PC_{[71]}BM$)	Experimental Optimum [ref.]
MDMO-PPV	262.2	2	80.7 (82.16)	80 [6]
APFO-Green5	1 091	1	72.75 (74.29)	67–75 [26]
pBTTT-C14	692.726	1	78.4 (79.9)	80 [14]
PCPDTBT	548.5634	≈ 2	72.68 (74.22)	67–75 [27]
PQT-C12	664.704	1	78.9 (80.4)	80 [21]
P3HT	166.18	N/A	50 (50)	50 [3]

domains of one material surround domains of the other to form a cul-de-sac and make it difficult for carriers to escape. It is likely that BHJ solar cells work best when they consist of a bicontinuous network with approximately equal volumes of electron-transporting (pure fullerene) and hole-transporting (intercalated phase or pure polymer) domains in order to have equal paths for electrons and holes and minimize the density of dead-ends. The fullerene weight percentage needed to match the volumes of the electron-transporting and the hole-transporting regions, assuming that the polymer and intercalated phase have the same density, is given by the equation

$$x = \frac{100 \cdot n \cdot \zeta + 50}{1 + n \cdot \zeta} \tag{1}$$

where ζ is the molecular weight ratio of the fullerene to the monomer and n is the number of fullerenes per monomer in the intercalated phase. This formula is derived in the Supporting Information section. The value of n was determined by the scale drawings of the chemical structures similar to Figures 1 and 4. If fullerenes cannot intercalate between the side-chains, $n = 0$. Table 2 compares the value of x for several polymer:fullerene BHJs to the experimentally optimized blending ratios found in the literature and shows that this simple formula consistently predicts the optimal blending ratio. This formula works despite not accounting for the fact that the fullerenes do not absorb light as well as the polymer because optimized devices are usually thick enough to have good absorption even with a high fullerene concentration.

3. Conclusions

We have shown that the side-chain spacing of several semicrystalline and amorphous semiconducting polymers allows for fullerene intercalation when sufficient free volume is present. In the case of pBTTT, we showed that a highly ordered, thermodynamically stable, bimolecular crystal is formed when the two materials were mixed and is composed of $PC_{[71]}BM$ intercalated between the side chains of pBTTT. These discoveries have several important implications. When intercalation occurs, a high level of fullerene-loading is necessary to create the phase separation needed for efficient BHJ solar cells, which leads to optimum blend ratios near 1:3-1:4 polymer:fullerene in contrast to an optimum near 1:1 in systems where intercalation cannot occur. We predict that the phase diagrams of polymer-fullerene blends will depend significantly on whether or not intercalation occurs. Our findings suggest that separate models of recombination will need to be developed for the two different kinds of cells that form depending on whether or not intercalation occurs. It is not yet clear if intercalation will be desirable as devices are engineered to operate near the theoretical efficiency limits. It will be necessary to adjust the position of fullerenes and other electron acceptors with different shapes and sizes to determine if intercalation is beneficial for solar energy conversion. However, it will be of general interest to use chemical design to intentionally create new bimolecular crystals of semiconducting molecules to tune the optoelectronic properties of the crystal by controlling the electronic coupling of neighboring molecules and to find ways to exploit these properties in novel optoelectronic devices such as solar cells, light-emitting diodes, LASERs, and biosensors.

4. Experimental

Substrate Preparation and Device Testing: Silicon substrates with a native oxide were coated with poly(3,4-ethylenedioxythiophene) poly(styrene sulfanate) (PEDOT:PSS) (Bayer AG) for the X-ray diffraction studies as this is similar to the standard substrate used in BHJs. For the TFT measurements, a 300-nm wet oxide was grown on a highly doped silicon substrates followed by immersion in octadecyltrichlorosilane (OTS) (Aldrich) (1 mM) in hexadecane yielding a contact angle of 105°. The films were formed by spin-casting a blend of the polymers and either $PC_{[61]}BM$ or $PC_{[71]}BM$ (nanoC) from either anhydrous 1,2-*ortho*-dichlorobenzene or chlorobenzene (Aldrich). The polymers were synthesized as previously reported (pBTTT, [7] pTT [17], and PQT [16]). All materials were used as received and every step after the application of PEDOT:PSS or OTS was performed inside a nitrogen glove box with less than 2-ppm oxygen. Top gold contacts with a 200-μm channel length were deposited for the TFT samples. Any annealing took place by placing the samples directly on a hotplate in the glove box for ten minutes. The pBTTT was annealed at 185 °C, the PQT at 140 °C, and the pTT at 240 °C

TFT measurements were performed in a vacuum probe station (MMR Technologies). For measurements of the electron (hole) mobility, the gate was biased positive (negative) in order to induce electrons (holes) at the film-OTS interface. The corresponding mobilities were calculated in the saturation regime ($|V_d| = 50$ V) using:

$$I_{ds} = \frac{W}{2L} C_i \mu \left(V_g - V_t\right)^2 \tag{2}$$

where I_{ds} is the source-drain current, W is the channel width, L is the channel length, C_i is the insulator capacitance ($C_i = 1.726 \times 10^{-8}$ F cm^{-2}), μ is the charge carrier mobility, V_g is the gate voltage, and V_t is the threshold voltage.

X-Ray Scattering: X-ray scattering experiments were carried out at the Stanford Synchrotron Radiation Laboratory (SSRL) on beamlines 2–1 (high resolution specular scattering) and 7–2 (high resolution grazing incidence scattering) at an energy of 8 keV, and on 11–3 (2D scattering with an area detector) at an energy of 12.7 keV. The grazing incidence measurements were taken on beamline 7–2 and 11–3 at the critical angle (0.2° on beamline 7–2 and 0.1° on beamline 11–3), the 2D GIXS was carried out at beamline 11–3 using the MAR345 image plate detector. All scattering was corrected for sample illumination and is expressed as a function of scattering vector, $\mathbf{q} = \mathbf{k}_{out} - \mathbf{k}_{in}$ [10].

WILEY InterScience DISCOVER SOMETHING GREAT
© 2009 WILEY-VCH Verlag GmbH & Co. KGaA, Weinheim

Acknowledgements

We would like to acknowledge Leslie Jimison, Alberto Salleo, Barry Thompson, Nicky Cates and Roman Gysel for fruitful discussions. Financial support was provided by Department of Energy (DOE) and the Global Climate and Energy Project at Stanford University (GCEP). Portions of this research were carried out at the Stanford Synchrotron Radiation Laboratory, a national user facility operated by Stanford University on behalf of the US Department of Energy, Office of Basic Energy Sciences. Supporting Information is available online from Wiley InterScience or from the author.

Received: November 3, 2008
Published online: March 2, 2009

[1] J. Y. Kim, S. H. Kim, H. H. Lee, K. Lee, W. L. Ma, X. Gong, A. J. Heeger, *Adv. Mater.* **2006**, *18*, 572.
[2] W. Ma, C. Yang, X. Gong, K. Lee, A. J. Heeger, *Adv. Funct. Mater.* **2005**, *15*, 1617.
[3] G. Li, V. Shrotriya, J. S. Yao, T. Moriarty, K. Emery, Y. Yang, *Nat. Mater.* **2005**, *4*, 864.
[4] A. C. Mayer, S. R. Scully, B. E. Hardin, M. W. Rowell, M. D. McGehee, *Mater. Today* **2007**, *10*, 28.
[5] B. C. Thompson, J. M. J. Frechet, *Angew. Chem. Int. Ed.* **2008**, *47*, 58.
[6] P. W. M. Blom, V. D. Mihailetchi, L. J. A. Koster, D. E. Markov, *Adv. Mater.* **2007**, *19*, 1551.
[7] M. C. Etter, P. W. Baures, *J. Am. Chem. Soc.* **1988**, *110*, 639.
[8] P. Srinivasan, T. Kanagasekaran, R. Gopalakrishnan, *Cryst. Growth Des.* **2008**, *8*(7), 2340.
[9] K. Tashiro, M. Kobayashi, T. Kawai, K. Yoshino, *Polymer* **1997**, *38*, 2867.
[10] J. J. Urban, D. V. Talapin, E. V. Shevchenko, C. R. Kagan, C. B. Murray, *Nat. Mater.* **2007**, *6*, 115.
[11] I. McCulloch, M. Heeney, C. Bailey, K. Genevicius, I. Macdonald, M. Shkunov, D. Sparrowe, S. Tierney, R. Wagner, W. M. Zhang, M. L. Chabinyc, R. J. Kline, M. D. McGehee, M. F. Toney, *Nat. Mater.* **2006**, *5*, 328.
[12] R. J. Kline, D. M. DeLongchamp, D. A. Fischer, E. K. Lin, L. J. Richter, M. L. Chabinyc, M. F. Toney, M. Heeney, I. McCulloch, *Macromolecules* **2007**, *40*, 7960.
[13] M. L. Chabinyc, M. F. Toney, R. J. Kline, I. McCulloch, M. Heeney, *J. Am. Chem. Soc.* **2007**, *129*, 3226.
[14] J. E. Parmer, A. C. Mayer, B. E. Hardin, S. R. Scully, M. D. McGehee, M. Heeney, I. McCulloch, *Appl. Phys. Lett.* **2008**, *92*, 113309.
[15] D. M. DeLongchamp, R. J. Kline, E. K. Lin, D. A. Fischer, L. J. Richter, L. A. Lucas, M. Heeney, I. McCulloch, J. E. Northrup, *Adv. Mater.* **2007**, *19*, 833.
[16] P. Brocorens, A. Van Vooren, M. Chabinyc, M. F. Toney, M. Shkunov, M. Heeney, I. McCulloch, J. Cornil, R. Lazzaroni. *Adv. Mater.*, in press.
[17] A. Swinnen, I. Haeldermans, M. van de Ven, J. D'Haen, G. Vanhoyland, S. Aresu, M. D'Olislaeger, J. Manca, *Adv. Funct. Mater.* **2006**, *16*, 760.
[18] M. Morana, P. Koers, C. Waldauf, M. Koppe, D. Muehlbacher, P. Denk, M. Scharber, D. Waller, C. Brabec, *Adv. Funct. Mater.* **2007**, *17*, 3274.
[19] E. J. Meijer, D. M. De Leeuw, S. Setayesh, E. Van Veenendaal, B. H. Huisman, P. W. M. Blom, J. C. Hummelen, U. Scherf, T. M. Klapwijk, *Nat. Mater.* **2003**, *2*, 678.
[20] M. Koppe, M. Scharber, C. Brabec, W. Duffy, M. Heeney, I. McCulloch, *Adv. Funct. Mater.* **2007**, *17*, 1371.
[21] B. C. Thompson, B. J. Kim, D. F. Kavulak, K. Sivula, C. Mauldin, J. M. J. Frechet, *Macromolecules* **2007**, *40*, 7425.
[22] Y. Kim, S. Cook, S. M. Tuladhar, J. Nelson, J. R. Durrant, D. D. C. Bradley, M. Giles, I. McCulloch, C. S. Ha, M. Ree, *Nat. Mater.* **2006**, *5*, 197.
[23] H. Hoppe, M. Niggermann, C. Winder, J. Kraut, R. Hiesgen, A. Hinsch, D. Meissner, N. S. Sariciftci, *Adv. Funct. Mater.* **2004**, *14*, 1005.
[24] C. R. McNeill, B. Watts, L. Thomsen, W. J. Belcher, A. L. D. Kilcoyne, N. C. Greenham, P. C. Dastoor, *Small* **2006**, *2*, 1432.
[25] Peter Peumans, Stanford University, private communication **2008**.
[26] F. Zhang, W. Mammo, L. M. Andersson, S. Admassie, M. R. Andersson, O. Inganas, *Adv. Mater.* **2006**, *18*, 2169.
[27] J. Peet, J. Y. Kim, N. E. Coates, W. L. Ma, D. Moses, A. J. Heeger, G. C. Bazan, *Nat. Mater.* **2007**, *6*, 497.

© 2009 WILEY-VCH Verlag GmbH & Co. KGaA, Weinheim